ON

NEUTRINO PHYSICS

D C Cundy

CERN

INTRODUCTION

During the past year essentially three main questions have been asked in neutrino physics:

1. Do neutral currents exist?
2. Do charged-current interactions scale up to high energy?
3. Is any "new" particle produced?

Judging from the submitted papers, the experimentalists have been very active over the last year in trying to answer these questions.

1. NEUTRAL CURRENT SEARCHES

For historical reasons and for clarity, I will divide the neutral current searches into "inclusive" and "exclusive" searches.

1.1 Inclusive Searches

1.1.1 GARGAMELLE-CERN Experiment

This heavy liquid bubble chamber experiment announced the first positive evidence[1] for neutral currents. In order to understand the new data that this group has presented it is essential to summarise briefly the old analysis. The experiment was carried out in a 3 m^3 fiducial volume inside a 7 m^3 visible volume. The liquid used was freon CF_3 Br, density 1.5. Three event types were defined:

(a) Neutral Current Candidates (NC) - These are events in which all the particles are positively identified as hadrons, and the total visible energy exceeds 1 GeV.

(b) Charged Current Candidates (CC) - These are events in which all tracks, except one, are positively identified as hadrons, the total energy of all the hadrons exceeds 1 GeV, and the remaining track is non-interacting and compatible with being a muon.

(c) Associated Events (AS) - These are events that would have been classed as NC candidates but for the fact that they are associated with a CC event having any amount of hadronic energy occuring in the same picture. They are attributed to charged-current neutrino events in which a high energy neutron is emitted and interacts in the chamber.

These events types are shown pictorially in Fig. 1. The results of the search can be summarised as follows:

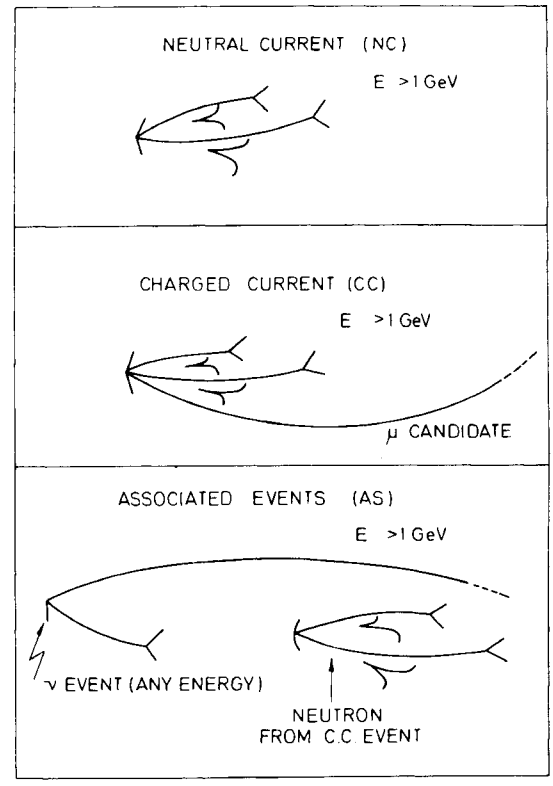

Fig. 1 Classification of event types in the GARGAMELLE experiment.

EVENT TYPE	ν	$\bar{\nu}$
NC	102	63
CC	413 (with μ^-)	113 (with μ^+)
AS	15	12
NC/picture	1.2×10^{-3}	0.3×10^{-3}

Note: NC/AS $\approx$ 6:1.

The question to be answered is whether these "NC" events are due to neutrons or neutrinos.

The first point to note is that the spatial distributions of the CC and NC events are identical. The sides of the chamber are well shielded by its magnet except at the ends and the neutron interaction length ($\sim$ 70 cms) is short compared with its length. Hence, if the NC events are due to neutrons they must be coming from neutrino interactions in the magnet.

If Gargamelle were situated in an infinitely large neutrino beam, and surrounded by an infinite shielding, then the neutrons and the neutrinos would be in equilibrium and the neutron background calculation would be analytical. The result would be:

$$\frac{NC}{AS} = \frac{1-\langle p \rangle}{\langle p \rangle}$$

where $\langle p \rangle$ is the probability that a neutron emitted from a CC event will interact. In the present experiment $\langle p \rangle \approx 0.5$, giving NC/AS $\approx$ 1 if all NC events were due to neutrons.

In practice, a Monte-Carlo calculation must be used which takes into account:

1. the actual layout of material around the bubble chamber;
2. the radial distribution of the neutrino flux;
3. the data on neutron production given by the AS events;
4. data on neutron interaction lengths in order to calculate cascade processes in the shielding.

This refined calculation gave a best value of NC/AS = 0.8 ± 0.4 corresponding to a neutron induced background of only $\sim$ 10%.

After small corrections for a contamination of NC events in the CC sample the published result was:

$$\left(\frac{NC}{CC}\right)_{\nu} = 0.23 \pm 0.03$$

$$\left(\frac{NC}{CC}\right)_{\bar{\nu}} = 0.46 \pm 0.09$$

The two main criticisms of this result were:

(a) the number of AS events on which the absolute neutron background calculation is based was too small (15 in ν film and 12 in $\bar{\nu}$ film) and could possibly be a statistical fluctuation.

(b) the neutron cascade processes in the material surrounding the chamber were perhaps not correctly understood.

The statistics have now been more than doubled for the neutrino film and the rate for the associated events is unchanged.

EVENTS/FILM		SEPTEMBER 1973	JULY 1974
NC/film	ν	$\frac{102}{111} = 0.92 \pm 0.13$	$\frac{189}{209} = 0.90 \pm 0.10$
	$\bar{\nu}$	$\frac{63}{276} = 0.23 \pm 0.01$	$\frac{70}{298} = 0.23 \pm 0.01$
AS/film	ν	$\frac{15}{111} = 0.13 \pm 0.04$	$\frac{42}{268} = 0.15 \pm 0.02$
	$\bar{\nu}$	$\frac{12}{276} = 0.04 \pm 0.01$	$\frac{14}{328} = 0.04 \pm 0.01$

(film $\equiv$ 750 photographs).

In order to investigate neutron cascade processes in detail, GARGAMELLE was exposed to protons of 4, 7 and 12 GeV. Except for small ionisation losses the behaviour of proton-initiated cascades and neutron-initiated cascades should be the same. The measured values of the interaction lengths and cascade lengths are shown in Fig. 2. They agree almost exactly with those used in the background calculation.

In addition at this conference the results of an "INTERNAL ANALYSIS" have been presented[2]. In this case the spatial distribution of the NC events has been used to estimate the neutron contamination. The momentum vector of the hadrons is taken as the line of flight of the incident neutral particle, thus allowing the length to the interaction (ℓ) and the potential length (L) to be calculated. Fig. 3 shows the data plotted in terms of $V = (1-e^{-\ell/\lambda})/(1-e^{-L/\lambda})$, where λ is the neutron interaction length. If the NC interactions were due to neutrons, then the V distribution would be flat. This is not the case. Furthermore, the NC and CC distributions are almost identical. It is possible to fit the observed NC distribution to obtain the neutron contamination. If x is the fraction of NC events due to neutrinos then:

$$(NC)_{observed} = x\ (NC)_{\nu} + (1-x)\ (NC)_{neutron}.$$

The results obtained are

$$x = 0.85^{+0.08}_{-0.10} \text{ for } \lambda_{neutron} = 70 \text{ cms}$$

and

$$x = 0.75^{+0.12}_{-0.18} \text{ for } \lambda_{neutron} = 100 \text{ cms}$$

agreeing with the previous background estimation.

Another internal check is to compare the pion charge ratio $r = \pi^{o}/(\pi^{+} + \pi^{-})$ for neutron induced and NC events. To increase the statistics on the neutron events, the AS events (which are neutron induced) have been combined with neutron events (NS) produced in the proton exposure. The results are given below as a function of the visible energy of the event.

E_{GeV}	r(AS + NS)	r(NC)
1-2	0.30 ± 0.07	0.75 ± 0.09
2-3	0.18 ± 0.06	0.53 ± 0.11
3-5	0.30 ± 0.08	0.37 ± 0.08
5-7	0.31 ± 0.16	0.48 ± 0.16

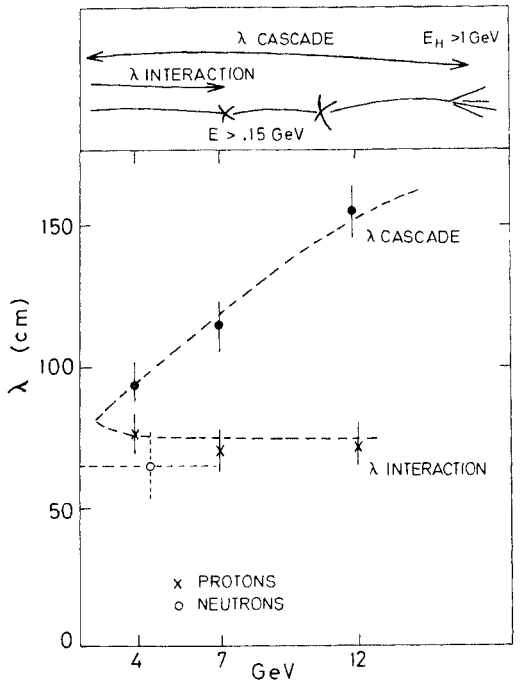

Fig. 2 Interaction length and Cascade length measurements in freon.

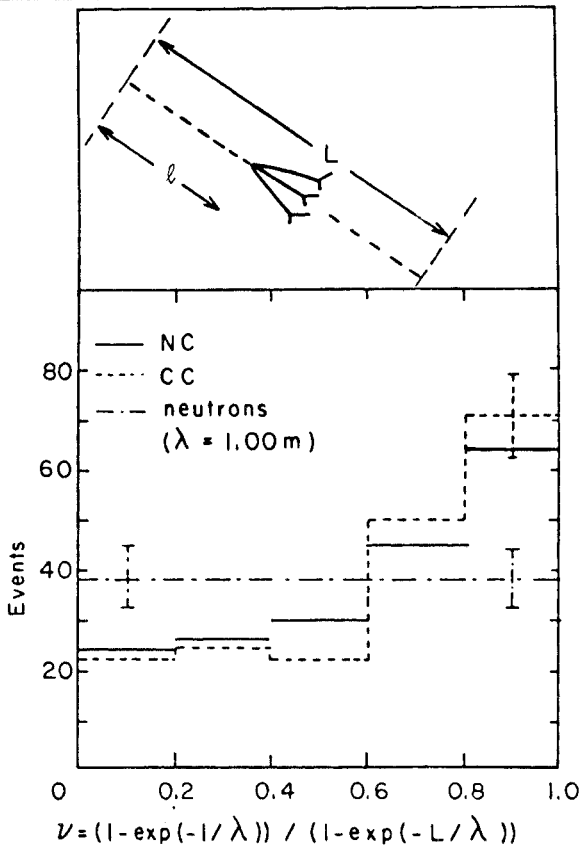

Fig. 3 The weighted interaction probability distributions for CC and NC events.

The χ^2 probability that these represent the same ratios is $\sim 10^{-4}$.

Therefore, the conclusions of this further analysis is that the initial analysis was correct and the latest values quoted for neutral currents in this experiment are:

$$R_\nu = \frac{NC}{CC}_\nu = 0.22 \pm 0.03$$

$$R_{\bar{\nu}} = \frac{NC}{CC}_{\bar{\nu}} = 0.43 \pm 0.12$$

1.1.2 FNAL HARVARD-PENNSYLVANIA-WISCONSIN Experiment

This experiment first presented evidence for neutral currents last September at the Bonn Conference[3]. The apparatus is shown schematically in Fig. 4. The target region consists of 70 tons of liquid scintillator, which is so large that it measures the total hadronic energy of neutrino events. In order to verticise neutrino events occurring in this calorimeter, it is divided into four by wide gap spark chambers SC1 - SC4. The calorimeter is followed by a muon detector. This consists of four iron toroids, 1.5 m thick, separated by spark chambers SC5 - SC8, thus allowing the sign of traversing muon to be determined.

In the Bonn paper the definition of a muon was any particle which traversed the first iron block of the muon detector.

The basis of the neutral current search is very simple. One finds the number of events with and without muons. From the events with muons one calculates the number of events in which the muon, though present, would not have been detected. One then asks whether there is an excess of muonless events.

Using an unfocused beam with a 3:1 $\nu:\bar{\nu}$ mixture, the result given at Bonn was:

Events with muon (CC) = 93

Events with no muon (NC) = 76

Calculated number of muonless events = 38

The relationship between the true ratio R = NC/CC and the measured ration R_m is

$$R = \varepsilon_\mu (1+R_m) - 1$$

where ε_μ is the muon detection probability.

In this case $\varepsilon_\mu = 0.71$, giving

$$R = 0.28 \pm 0.10.$$

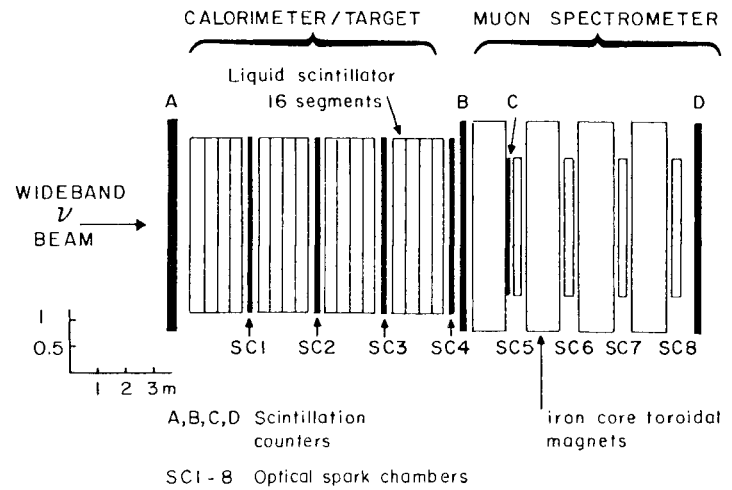

Fig. 4 Apparatus of the FNAL Harvard-Pennsylvania-Wisconsin (HPW) experiment.

The main criticism of this experiment was its sensitivity to ε_μ: for $\varepsilon_\mu = \frac{1}{1+R_m} = 0.55$ then R is zero!

For the next series of experiments the apparatus was modified by introducing a 35 cm thick iron slab between the end of the calorimeter and SC4 and counter B. Also the area of the spark chambers in the muon identifier was increased from 5.3 to 13.4 m^2; thus increasing the muon detection efficiency.

In this set-up there are three definitions of a muon:

(i) μ_1 a particle firing counter B,

(ii) μ_1 a particle observed in SC4,

(iii) μ_2 a particle firing counter C (i.e. the old definition).

Because the 35 cm of iron cannot always stop a hadron shower, the relationship between the true ratio R = NC/CC and the measured ratio R_m becomes more complicated.

It is in fact:

$$R = \frac{(\varepsilon_\mu + \varepsilon_p - \varepsilon_\mu\varepsilon_p)\ (1 + R_m)-1}{1 - \varepsilon_p\ (1 + R_m)}$$

where ε_p is the probability that the hadron in an event will "punch through" and simulate a muon.

Therefore, the experiment is now sensitive to ε_p as well as ε_μ.

ε_p was determined by using the hadron showers in CC events in which the muon is definitely identified in the muon identifier.

The muon detection efficiency is determined from the observed CC events assuming azimuthal symmetry.

Experiments were performed in beams having different admixtures of ν and $\bar{\nu}$ hence:

$$R = R_{\bar{\nu}}\ (1-\alpha) + \alpha\ R_\nu$$

where $\alpha = CC_\nu/(CC_\nu + CC_{\bar{\nu}})$.

The results of these different experiments are summarised below

SAMPLE	NUMBER OF EVENTS	α	R
Wide band Horn off	255	0.74	0.18 ± 0.05
Wide band Horn on	283	0.45	0.22 ± 0.05
Narrow band $(\pi,K)^-$ selected	100	0.12	0.34 ± 0.12
Narrow band $(\pi,K)^+$ selected	188	0.98	0.13 ± 0.06

The combined best values for R_ν and $R_{\bar{\nu}}$ are quoted as:

$$R_\nu = 0.12 \pm 0.04$$

$$R_{\bar{\nu}} = 0.32 \pm 0.08$$

1.1.3 FNAL, CALTECH-Experiment[5]

This experiment has been carried out in narrow band ν and $\bar{\nu}$ beams. The apparatus is shown schematically in Fig. 5. It consists of a $\sim$ 120 ton calorimeter composed of 10 cm thick iron-spark chamber-counter modules. The calorimeter is followed by a toroidal iron magnet for muon identification.

The basic idea behind the neutral current search is again very simple. A muon travels $\sim$ 1 metre/GeV in iron, whilst a 100 GeV hadron shower travels $\sim$ 1 metre. Therefore, the penetration depth of neutral current events and charged current events will be different. Demanding a minimum energy

deposit of 6 GeV in the calorimeter, the projected length of the most penetrating particle of an event is measured. Fig. 6 shows the length distribution for events produced in the ν beam. A large peak is noticed at small lengths. In order to calculate the length distribution expected from charged current events with large angle muons, events with projected length > 1.4 metres were taken as charged-current events. Assuming scaling behaviour, it is possible to estimate this background, as shown in Fig. 6. Similarly, the background from the wide-band component of the beam, which comes from disintegrations before the momentum analysis, is also shown. It is clear that the observed distribution cannot be ascribed to charged-current events. Fig. 7 shows the results for the $\bar{\nu}$ exposure.

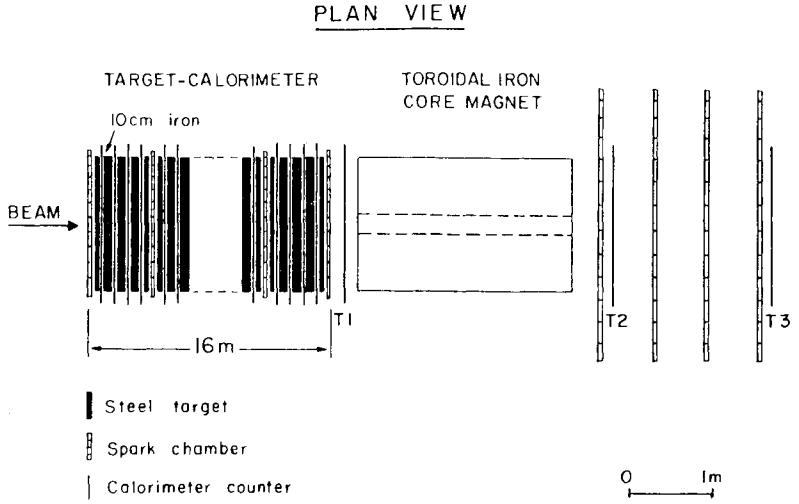

Fig. 5 Apparatus of the FNAL CALTECH experiment.

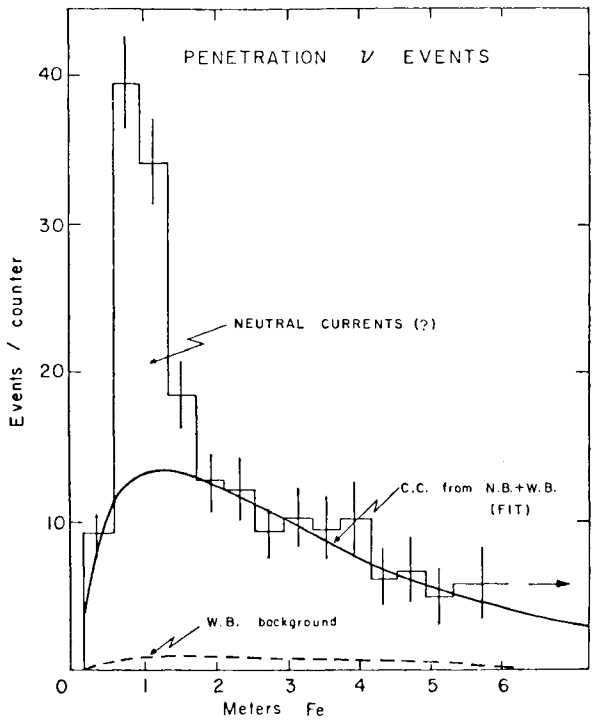

Fig. 6 Penetration distribution for events produced in neutrino beam.

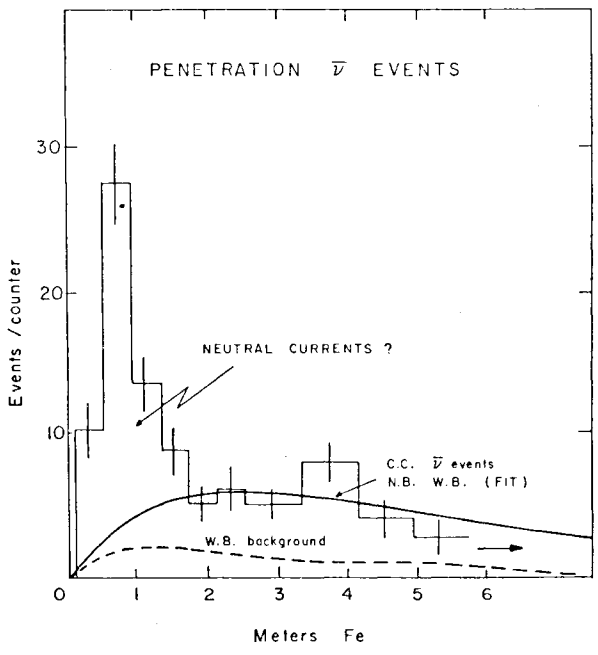

Fig. 7 Penetration distribution for events produced in anti-neutrino beam.

Before attributing this excess of events to neutral currents several questions must be answered.

1. Are they due to neutrons?
   No, the spatial distribution of the events in the peak is flat throughout the calorimeter.

2. Are they due to a very low energy background coming from the wide-band component of the beam?
   This was checked by shutting the momentum slit and running with only this wide-band component present. The number of events was found to be within a factor of two of the estimated value.

3. Are the events due to anomalous (i.e. non-scaling) charged current events with low energy, large angle muons?
   If this were the case the hadron energy of these events should be high. Fig. 8 shows the energy distribution of the neutral current candidates. It is certainly not peaked to high energy, and for comparison the charged-current background (assuming scaling) is shown.

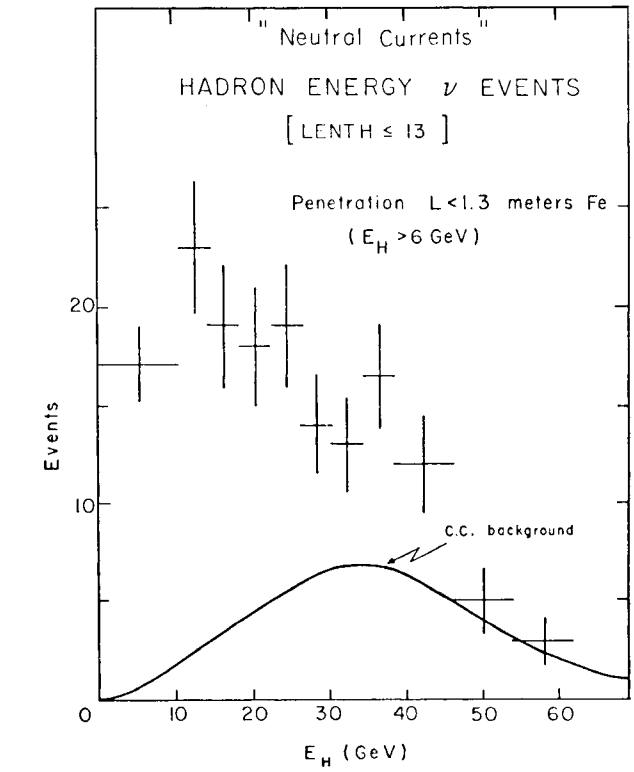

Fig. 8 Energy distribution for "neutral current" candidates (penetration lengths < 1.3 metres F_e).

The final results are shown below:

FOR NEUTRINO

PENETRATION LENGTH (metres)	EVENTS OBSERVED	CHARGED CURRENT ESTIMATION
1.4 - ∞	666	666
1.4 - 6.0	371	412
0.0 - 1.4	332	155

Giving: $R_\nu = \frac{177}{821} = 0.22.$

FOR ANTI-NEUTRINO

PENETRATION LENGTH (metres)	EVENTS OBSERVED	CHARGED CURRENT ESTIMATION
1.4 - ∞	444	444
1.4 - 6.0	207	171
0.0 - 1.4	202	41

Giving: $R_{\bar{\nu}} = \frac{161}{485} = 0.33.$

The authors of this experiment consider that these results should be taken mainly as a demonstration of the existence of neutral currents and emphasize that not until the actual structures of both the charged and neutral current processes have been measured can a true NC/CC ratio be given.

However, for historical reasons I show all three neutral current results in Fig. 9, along with the lower bound calculated[6] using the Weinberg-Salam model. The errors are such that both results are compatible with the ratios being energy dependent

or not. Perhaps a more pertinent question to ask is what are the neutral current cross-section ratios?

These I estimate to be:

$$\frac{\sigma^{o}_{\nu}}{\sigma^{o}_{\bar{\nu}}} = 0.5 \pm 0.2 \text{ Gargamelle}$$

$$\frac{\sigma^{o}_{\nu}}{\sigma^{o}_{\bar{\nu}}} = 1.0 \pm 0.2 \text{ HPW.}$$

If one assumes a specific model, in particular the quark-parton model[7], the Gargamelle result can be used to estimate the Weinberg angle. The result is

$$\sin^2 \theta_w = 0.39 \pm 0.05.$$

However, this result should be treated with a certain caution as the charged current energy transfer distribution certainly does not agree with the parton model predictions.

1.2 Neutral Current Searches in Specific Channels

It is only by the investigation of specific channels that the true nature of the "neutral current" phenomena will be understood, and experimentally there is quite an activity in this respect.

1.2.1 CERN-GARGAMELLE $\bar{\nu}_\mu + e^- \rightarrow \nu_\mu + e^-$ Search

This process, because it is not complicated by hadronic effects is certainly the best possible way of investigating the neutral current process. Experimentally, at the CERN PS energies, it is certainly a very clean experiment. However, it does suffer from the problem of very low rate.

The signal, single electrons, should all be found at a small angle θ_e to the neutrino beam direction:

$$\theta_e < \sqrt{\frac{2m_e}{E_e}}$$

which for $E_e > 300$ MeV (a historical scanning cut!) gives $\theta_e < 3^o$.

This is about the same as the angular resolution for electron measurements, so candidates are accepted up to angles $< 5^o$. To date 2 events have been observed.

The background comes from two sources:

(a) The main background process is $\nu_e + n \rightarrow e^- (< 5^o) + p$ (not seen). This is estimated by using the equivalent reaction with ν_μ. It was found that only 1.7% of events of the type $\nu_\mu + n \rightarrow \mu^- + p$ had a configuration corresponding to such a background. Using the ν_e flux estimate, which is only $\sim 0.1\%$ of the $\bar{\nu}_\mu$ flux, the background from

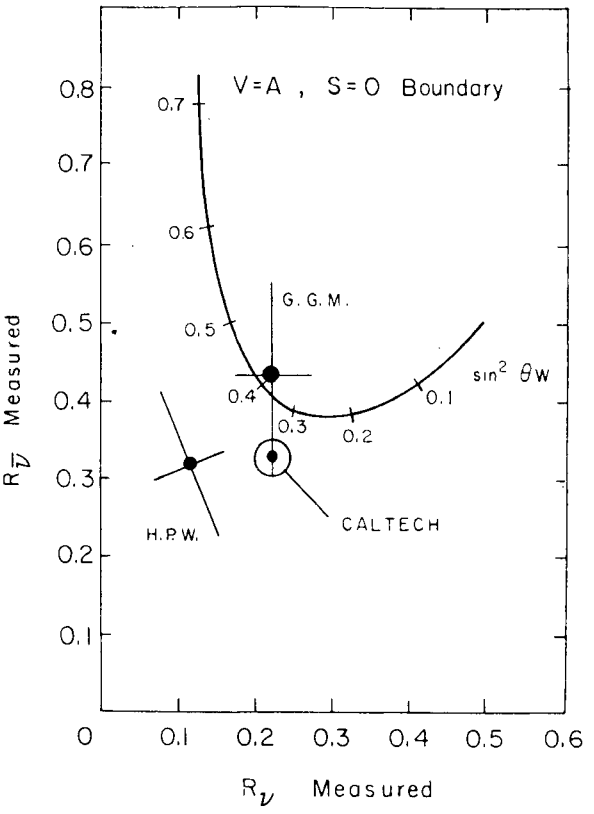

Fig. 9 Comparison of the measurements of R_ν and $R_{\bar{\nu}}$ with the lower theoretical bound.

this process is estimated to be 0.12 ± 0.08 events.

(b) The other source of background comes from γ rays emitted in forward direction. Three isolated electron-positron pairs are seen with angles < 5° to the neutrino beam direction. As only ∿ 2% of electron-positron pairs will be confused with electrons, the background is estimated to be 0.06 ± 0.03 events.

Hence, the final result is a 2 events signal with a 0.18 ± 0.12 event estimated background.

This result can be used to set limits on the cross-section for the process

$$\bar{\nu}_\mu + e^- \rightarrow \bar{\nu}_\mu + e^-$$

Upper limit $0.30\ E_{\bar{\nu}} \times 10^{-41}$ cm²/el

Lower limit $0.03\ E_{\bar{\nu}} \times 10^{-41}$ cm²/el

90% C.L.

In terms of the Weinberg-Salam model as calculated by t'Hooft[8] the result gives $\sin^2 \theta_w < 0.45$ (90% C.L.).

1.2.2 ANL Single Pion Production Neutral Current Search[9]

This experiment was carried out in the ANL 12' bubble chamber using 0.36 x 10^6 pictures in hydrogen and 0.40 x 10^6 pictures in deuterium, with an average of 1.3 x 10^{12} protons per pulse.

The experiment looks for the reactions:

$$\nu p \rightarrow \nu n \pi^+$$
$$\nu p \rightarrow \nu p \pi^o$$
$$\nu n \rightarrow \nu p \pi^-$$

relative to $\nu p \rightarrow \mu^- p \pi^+$. The neutron flux which gives rise to the background was measured directly by picking up the reaction $np \rightarrow pp\pi^-$ (a 1-C fit). This cross-section is equal to that of the reaction $np \rightarrow nn\pi^+$. In addition, it should be noted that for neutrons energies up to 3-4 GeV (which is the case in the experiment) the momentum distribution of the π^+ and π^- are the same.

The relationship between the reactions giving $pp\pi^-$, $np\pi^o$, $np\pi^-$ final states was determined by means of a separate neutron exposure.

The neutrons were observed to come from the top of the chamber. By applying momentum cuts on the proton (< 1 GeV/c) and the charged pions (< 400 MeV/c), and also dip cuts on the π^+ and proton, it was found possible to eliminate the neutron background almost completely. A photo-production background due to γ rays from cosmic muons was eliminated by demanding that all events be more than 20 cms from a cosmic ray.

The final results are:

	NUMBER OF EVENTS	BACKGROUND
$\nu p \rightarrow \nu n \pi^+$	7	0.9 ± 0.5
$\nu p \rightarrow \nu p \pi^o$	7	1.6 ± 0.5
$\nu n \rightarrow \nu p \pi^-$	14	2.0 ± 2.0
	28	4.5 ± 2.2

These data give the following ratios:

$$\frac{\nu p \pi^o}{\bar{\mu} p \pi^o} = 0.51 \pm 0.27$$

$$\frac{\nu n \pi^+}{\bar{\mu} p \pi^+} = 0.17 \pm 0.08$$

} 0.68 ± 0.28

$$\frac{\nu p \pi^-}{\bar{\mu} p \pi^+} = 0.18 \pm 0.07$$

The results on π^+ and π^o production, compared with the theoretical predictions[10] as a function of $\sin^2 \theta_w$, are shown in Fig. 10. The theoretical prediction is very sensitive to the relative amounts

of $I = \frac{1}{2}$, $I = \frac{3}{2}$ present in the transition. That there is a large $I = \frac{1}{2}$ non-resonant contribution in single pion production is indicated from the $\pi^- p$ invariant mass plot.

1.2.3 CERN Propane Bubble Chamber (1967) Re-analysis[11]

In 1970 this experiment published[12] only an upper limit for the process $\nu p \to \nu n \pi^+$ since no estimate was made of the neutron background.
A search has now been made for events topologically compatible with the reaction $np \to pp\pi^-$, and none was found. The result of this experiment is:

$$\frac{\nu n \pi^+}{\mu^- p \pi^+} = \frac{8}{67} = 0.12 \pm 0.06$$

Note that about one half of these events are on carbon and the ratio is modified by charge exchange effects.

1.2.4 BROOKHAVEN-COLUMBIA Spark Chamber Experiment[13]

This is a very recent experiment using a thin plate aluminium spark chamber system. Tracks originating in the system were classified into five categories:

1) clear muon (straight track > 2 interaction lengths),
2) leaving straight track,
3) stopping straight track,
4) interacting track (kink or shower),
5) short track (i.e. $\lesssim$ 8 cms).

Muonless events (Neutral Current or NC) were defined as events with tracks of types 4) and 5) only. Charged current events (CC) were defined as events having a track of type 1) in addition. 111 CC events were observed, which after correction for loss of large angle muons becomes 130. A total of 45 NC were observed, therefore demonstrating a large neutral current signal.

A sub-sample of events with single π^0 production have been selected giving:

$$\frac{\nu N' \pi^0}{2(\mu^- N' \pi^0)} = 0.14 \pm 0.07$$

where N' is the aluminium nucleus. The interpretation of this ratio is complicated by charge exchange effects.

1.3 Conclusions on the Neutral Current Searches

(i) ν_μ beams can interact with matter without producing a muon.

(ii) At present no evidence exists for not attributing them to neutral currents rather than something more exotic.

(iii) The structure of the neutral current has yet to be determined.

2. CHARGED CURRENT INTERACTIONS

If neutrino interactions scale, then for iso-scalar targets the differential cross-section is given by:

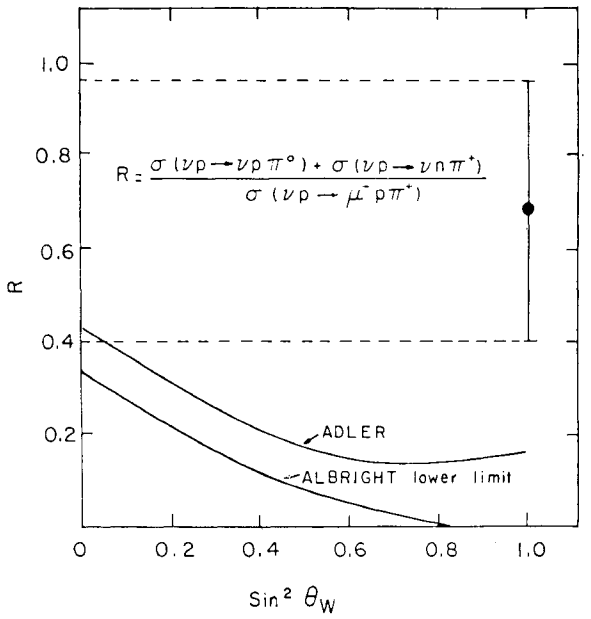

Fig. 10 Comparison of single π^+, π^0 production with theoretical estimates.

$$\frac{d^2\sigma}{dxdy} = \frac{G^2ME}{\pi}\left\{(1-y)F_2(x) + \frac{y^2}{2}\ 2xF_1(x) \pm y(1-\frac{y}{2})\ xF_3(x)\right\}$$

where x and y are the Bjorken scaling variables defined by $x = q^2/2M\nu$ and $y = \nu/E$

(q^2 = four-momentum transfer

ν = energy transfer to the hadron system

E = incident neutrino energy

M = nucleon mass)

2.1 Total Cross-sections

The most important consequence of the above formula is that it predicts a neutrino cross-section which rises linearly with energy. Defining

$$A = \frac{\int_0^1 2x\ F_1(x)dx}{\int_0^1 F_2(x)dx}\ , \text{ and } B = \frac{\int_0^1 xF_3(x)dx}{\int_0^1 F_2(x)dx}$$

then the relationship between the ν and $\bar{\nu}$ cross-sections is given by:

$$R = \frac{\sigma(\bar{\nu})}{\sigma(\nu)} = \frac{3+A-2B}{3+A+2B}$$

In addition, there is the positivity condition

$$|B| \leq A \leq 1.$$

Results on the total ν and $\bar{\nu}$ cross-sections have been presented by the GARGAMELLE[14], CALTECH[15], and the HPW[16] experiments, and are shown in Figs. 11 and 12.

The slopes quoted by each experiment along with the estimated error (which are mainly flux errors) are:

	ν	$\bar{\nu}$
GARGAMELLE	0.76 ± 0.08 (10%)	0.28 ± 0.03 (10%)
CALTECH	0.83 ± 0.11 (13%)	0.28 ± 0.05 (18%)
HPW	0.70 ± 0.13 (25%)	0.28 ± 0.09 (30%)
Mean	0.78 ± 0.07	0.28 ± 0.025

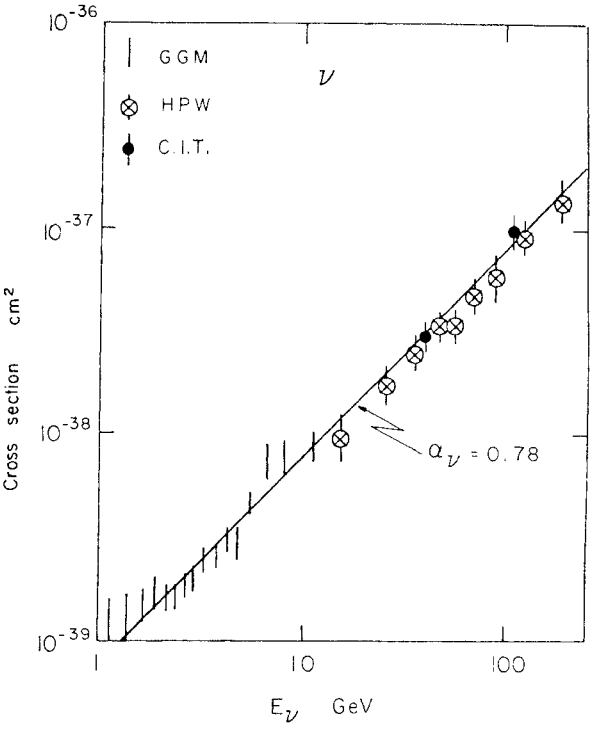

Fig. 11 Measurements of the total charged-current ν cross-section.

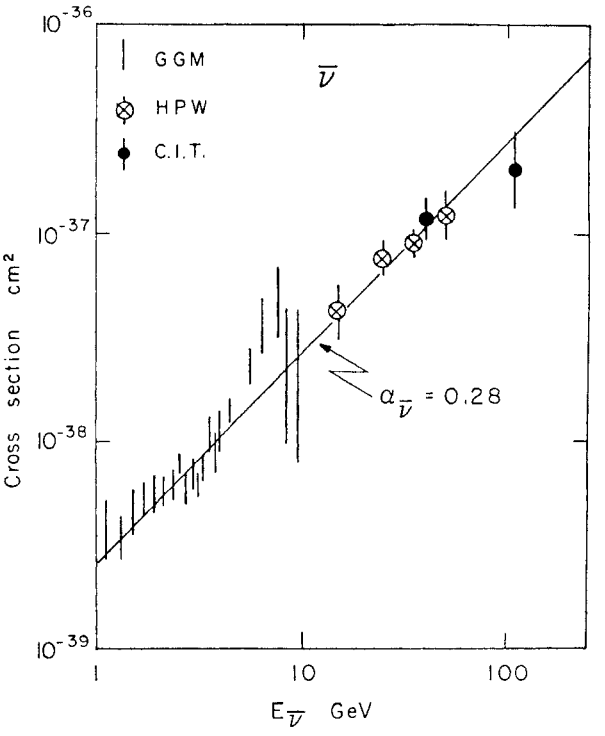

Fig. 12 Measurements of the total charged-current $\bar{\nu}$ cross-section.

The agreement between the slopes is striking and taking the mean of the three results probably has some sense.

In each experiment the determination of the ratio $R = \sigma(\bar{\nu})/\sigma(\nu)$ is more accurate than the slope determination because systematic effects in the flux determination cancel out.

	ENERGY REGION	R
GARGAMELLE	1-10 GeV	0.38 ± 0.02
CALTECH	40 GeV	0.40 ± 0.11
	110 GeV	0.23 ± 0.11
HPW	10-30 GeV	0.41 ± 0.11

A value of R estimated from the slopes is $R = 0.36 \pm 0.05$. This gives limits on the value of A:

$$1 \geq A \geq 0.92 \ (\pm 0.1)$$

Note that A = 1 implies that all the neutrino scattering takes place on spin $\frac{1}{2}$ constituents.

Similarly, the limits of B are:

$$0.94 \geq B \geq 0.92 \ (\pm 0.1)$$

It is instructive to digress somewhat on the actual meaning of B. This is best understood in terms of the spin $\frac{1}{2}$ parton model.

In this model the differential cross-sections are very simple:

$$\frac{d^2\sigma_\nu}{dxdy} = \frac{G^2ME}{\pi}\left[q(x) + \bar{q}(x)(1-y)^2\right]$$

$$\frac{d^2\sigma_{\bar{\nu}}}{dxdy} = \frac{G^2ME}{\pi}\left[\bar{q}(x) + q(x)(1-y)^2\right]$$

where

$$q(x) = x\,n(x) \qquad \text{partons}$$

$$\bar{q}(x) = x\,\bar{n}(x) \qquad \text{anti-partons}$$

n(x) being the probability that the parton takes a fraction x of the nucleon four-momentum. Therefore, one obtains the very simple relationships:

$$F_2(x) = q(x) + \bar{q}(x)$$

$$xF_3(x) = q(x) - \bar{q}(x)$$

Defining $Q = \int_0^1 q(x)\,dx$, then $\bar{Q}/(Q+\bar{Q}) = (1-B)/2 \leq 10\%$ (90% confidence). That is B measures the amount of anti-matter in the nucleon.

The sum of the neutrino and anti-neutrino cross-sections measures $F_2(x)$, as the interference term $F_3(x)$ drops out:

$$\sigma^{\nu N} + \sigma^{\bar{\nu}N} = 4\,\frac{G^2ME}{\pi}\int F_2^{\nu N}\,dx$$

$$= 1.04 \pm 0.08$$

giving $\int F_2^{\nu N}\,dx = 0.51 \pm 0.05$.

The relationship between $F_2^{\nu N}$ and F_2^{eN} measures the mean square charge of the constituents.

The fractional quark model prediction is $\int F_2^{\nu N}dx \leq \frac{18}{5}\int F_2^{eN}dx$ (the equality being true if there are no strange constituents). Experimentally we have

$$\int F_2^{\nu N}\,dx = 0.51 \pm 0.05$$

$$\frac{18}{5}\int F_2^{eN}\,dx = 0.51 \pm 0.08$$

2.2 Differential Distributions

As the total cross-section data seem to be in such good agreement with the scaling predictions, it is interesting to see if this is also true of the differential x and y distributions.

2.2.1 y Distributions

The scaling region, as described by the SLAC

results, is the region $q^2 > 1$ GeV^2 and $W^2 > 4$ GeV^2 (where W is the mass of the hadronic system).

The GARGAMELLE experiment[14], because it is at low energy, has very little of its data in this region. However, the small amount which is (232 ν and 42 $\bar{\nu}$ events) is shown in Fig. 13. The y distributions for ν and $\bar{\nu}$ interactions are certainly compatible with those expected for B = 0.9, as found from the cross-section data.

The CALTECH data[17] are shown in Fig. 14. As the target calorimeter is very long, the muon acceptance falls rapidly with increasing y. Because of this, the group use only data up to y = 0.6, and fit a distribution of the type $dN/dy = c(1+a(1-y)^2)$. In this case $a = \bar{Q}/Q$, and the best fit obtained is $a = +0.05^{+0.25}_{-0.17}$. This is to be compared with $0.03 \leq (1-B)/2 \leq 0.04$ ($\pm$ 0.05) obtained from the cross-sections.

The HPW data[18] divided into energy values above and below 30 GeV are shown in Fig. 15. The curves drawn correspond to B = 1 (i.e. no antiparton contribution). The agreement with the neutrino data is good. However, a large discrepancy seems to show up in the anti-neutrino data. The y distributions for $\bar{\nu}$ are much the more sensitive to any anti-parton contribution as the latter will add a flat distribution to the rapidly falling $(1-y)^2$ distribution. As pointed out by B. Barish (CALTECH), this is considerably amplified when the detector has limited angular acceptance. If the detector has a mean muon angular acceptance of $\langle\theta\rangle$, the maximum x value which can be measured is given by:

$$x_{max} = \frac{(1-y)\, E\langle\theta\rangle^2}{2My}$$

where E is the neutrino energy.

The expected y distribution for $\bar{\nu}$ is then

$$\frac{dN_{\bar{\nu}}}{dy} = c. \int_0^{x_{max}} q(x)dx \left[(1-y)^2 + \frac{\int_0^{x_{max}} \bar{q}(x)dx}{\int_0^{x_{max}} q(x)dx} \right]$$

where x_{max} approaches zero as y approaches 1.

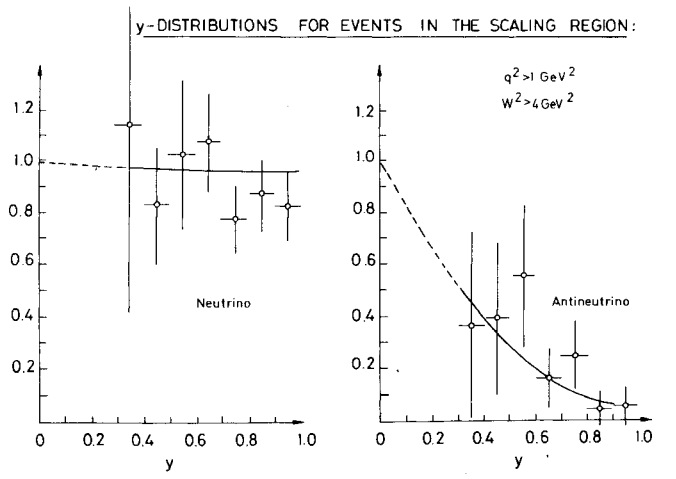

Fig. 13 GARGAMELLE-y-distributions for events in the scaling region $q^2 > 1$ GeV^2, $W^2 > 4$ GeV^2.

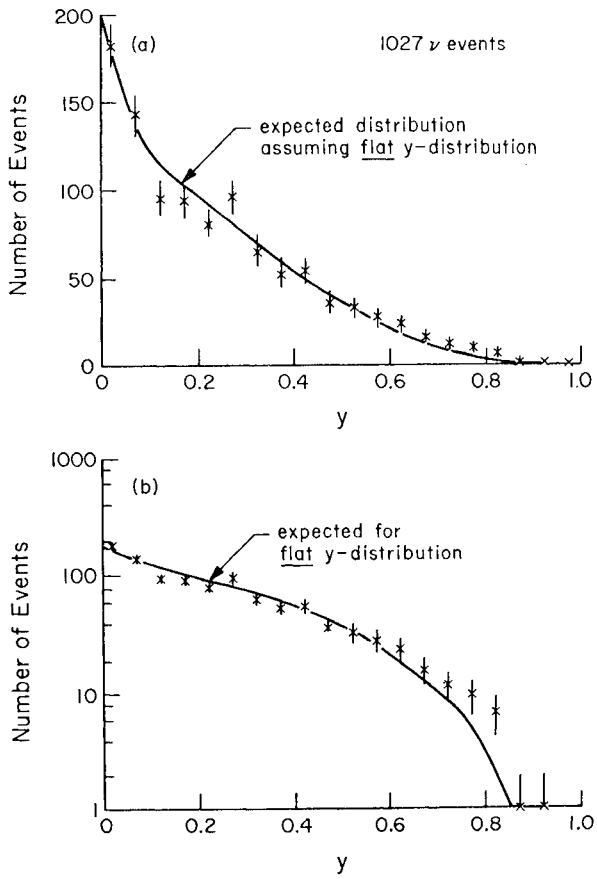

Fig. 14 FNAL CALTECH measured y distributions.

Depending on the form of the $\bar{q}$ distribution, the size of the second term can become large with respect to the $(1-y)^2$ term. Therefore, until a complete analysis has been performed on this data, it is not possible to say how large, if any, is the disagreement(*).

2.2.2 x-Distribution

Using the sum and the difference of the measured $d\sigma(\bar{\nu})/dx$ and $d\sigma(\nu)/dx$ distributions it is possible to extract the structure functions $F_2(x)$ and $xF_3(x)$. Fig. 16 shows these structure functions obtained from the GARGAMELLE experiment, using only data in the SLAC scaling region. Again one notes the agreement with the fractional quark model predictions for the comparison of neutrino and electro-production structure functions.

This agreement was found at higher energy by the CALTECH experiment as is shown in Fig. 17. This figure also demonstrates the difficulty such counter experiments have in determining the structure functions due to the acceptance problems.

(*) During the preparation of the written version of this talk, a private communication from the HPW group indicates that after correcting for the angular acceptance, discrepancy still exists in the $\bar{\nu}$ data. However, it is only present for $x < 0.1$ and $y > 0.6$. This could possibly indicate the opening up of a new channel.

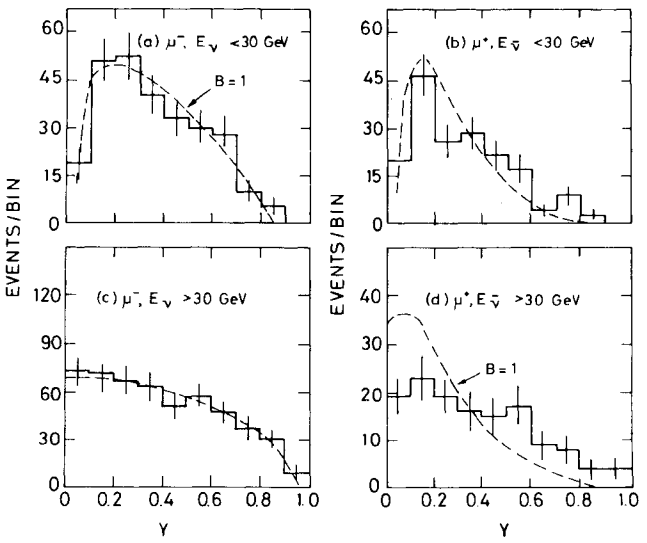

Fig. 15 FNAL HPW measured y distributions.

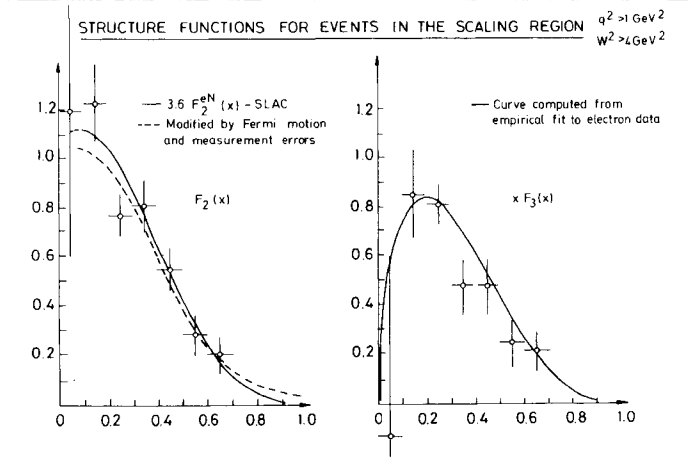

Fig. 16 GARGAMELLE-structure functions for events in the scaling region $q^2 > 1$ GeV^2, $W^2 > 4$ GeV^2.

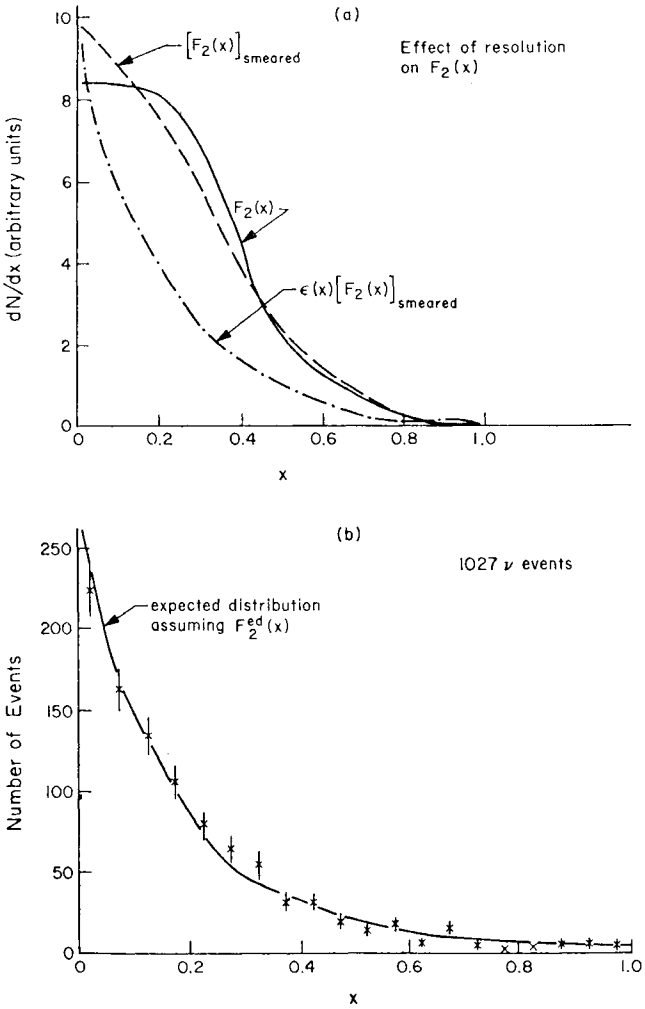

Fig. 17 FNAL CALTECH x distributions.

2.3 Precocious Scaling

Because of the large amount of data in the non-scaling region, the GARGAMELLE group have looked for ways of extending the use of the structure functions into the resonance production region and the region $q^2 < 1.0$ GeV^2. New structure functions were empirically defined as:

$$\tilde{F}_2(x') = \frac{3\pi}{4G^2E}\left[\frac{d\sigma(\nu)}{dx'} + \frac{d\sigma(\bar{\nu})}{dx'}\right]$$

$$x\tilde{F}_3(x') = \frac{3\pi}{2G^2E}\left[\frac{d\sigma(\nu)}{dx'} - \frac{d\sigma(\bar{\nu})}{dx'}\right]$$

where $x' = q^2/2M\nu + M^2$ is the Bloom-Gilman scaling variable.

In electro-production, the use of x' allowed the extension of scaling into the resonance region, but only for $q^2 > 1.0$ GeV^2.

In defining the structure functions in this way the y distributions, which do not scale, are integrated experimentally. The y distributions in the resonance region would not be expected to scale because resonance production will take place mainly at small y.

The structure functions $\tilde{F}_2(x')$ are shown in Fig. 18 for various energy regions. The agreement with the SLAC structure functions is good at all energies. Encouraged by this, the GARGAMELLE group have extracted $\tilde{F}_3(x')$ and its integral, as a function of energy. $\int_0^1 \tilde{F}_3(x')\,dx'$, the Gross-Llewellyn-Smith Sum Rule[18], can be physically interpretated as being equal to the number of matter constituents minus the number of anti-matter constituents in the nucleon.

For the fractional quark model, the prediction for the neutron-proton mixture in freon is 3.1.

Fig. 19 shows the value of the integral as a function of energy. The mean value is:

$$\int_0^1 \tilde{F}_3(x')\,dx' = 3.2 \pm 0.6$$

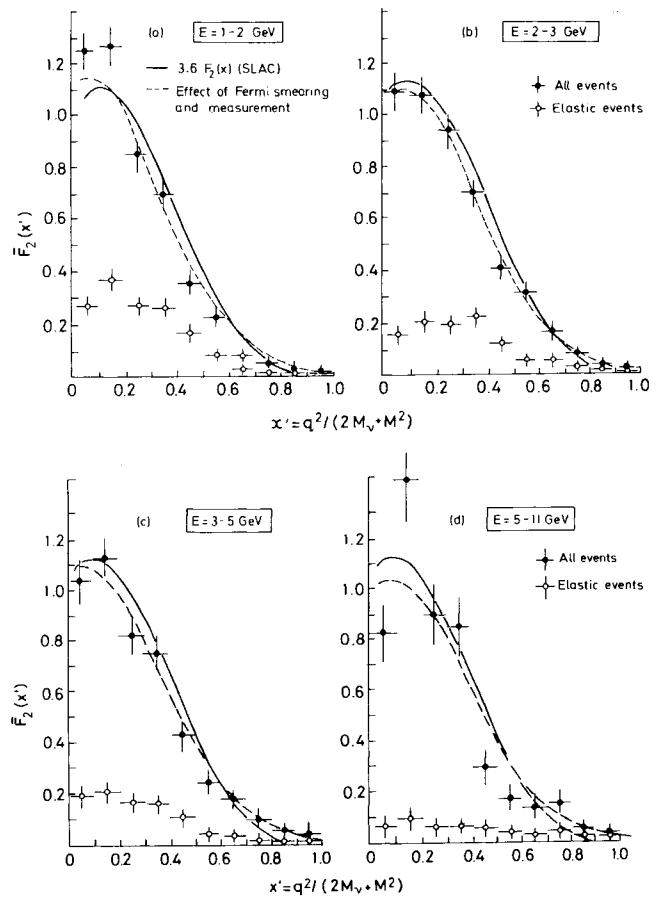

Fig. 18 GARGAMELLE-$\bar{F}_2(x')$ determined at various neutrino energies.

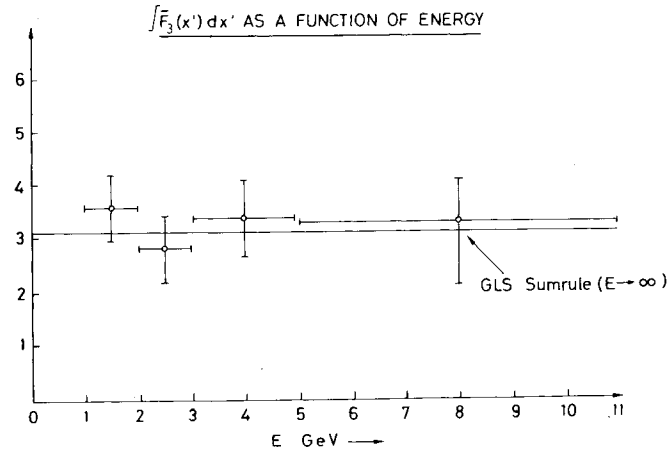

Fig. 19 GARGAMELLE-evaluation of $\int \tilde{F}_3(x')dx'$ as a function of neutrino energy.

As stated earlier, in terms of the parton model, $F_2(x)$ and $F_3(x)$ can be used to determine the momentum distribution of the constituents. Fig. 20 shows the experimental distribution. These are compared with theoretical predictions[20] which use empirical fits to the electro-production data and Regge-like behaviour for the lepton-quark scattering.

Finally, the GARGAMELLE group have looked at the ratio of π^+/π^- production. According to the parton model, the differential cross-section for producing a pion taking a fraction z of the total hadronic energy (i.e. $z = E_\pi/E_{hadron}$) is given by:

$$\frac{d^2\sigma_\nu^{\pi^+}}{dx\,dz} = c.x. \left[d(x)\, D_u^{\pi^+}(z) + \frac{1}{3}\bar{u}(x)\, D_{\bar{d}}^{\pi^+}(z) \right]$$

and

$$\frac{d^2\sigma_\nu^{\pi^-}}{dx\,dz} = c.x. \left[d(x)\, D_u^{\pi^-}(z) + \frac{1}{3}\bar{u}(x)\, D_{\bar{d}}^{\pi^-}(z) \right]$$

where $d(x)$ and $\bar{u}(x)$ are the probability distributions of isospin down partons and anti-partons, and $D_u(z)$ is the probability of a parton decaying into a π^+ taking a fraction z of the total hadronic energy.

Charge symmetry gives

$$D_u^{\pi^+} = D_{\bar{d}}^{\pi^+}$$

$$D_u^{\pi^-} = D_{\bar{d}}^{\pi^-}$$

Hence

$$R\left(\frac{\pi^+}{\pi^-}\right) = \frac{D_u^{\pi^+}(z)}{D_u^{\pi^-}(z)} \quad \text{independent of x.}$$

In ν interactions, a μ^- must be produced. Hence, the π^+/π^- ratio must, by charge conservation, become infinite as $z \to 1.0$.

In addition, for the simple parton model of current fragmentation to be valid, one demands $z > 0.3$. Hence, only the experimental data in the region $0.3 < z < 0.7$ have been used. These data are shown in Fig. 21 and are compared with the theoretical prediction[21], obtained from electro-production data.

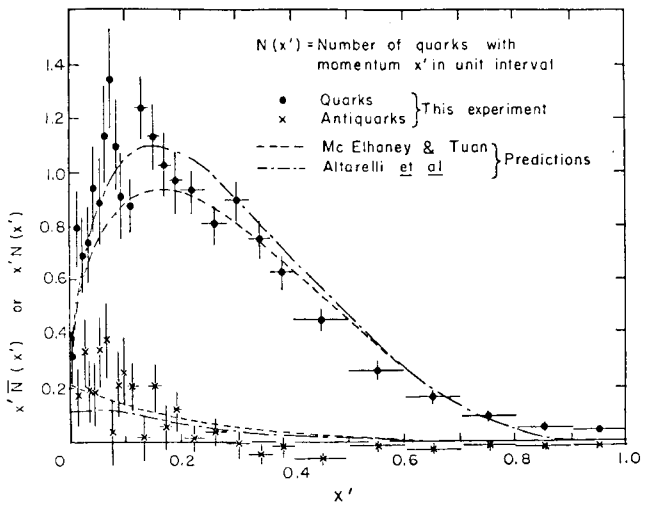

Fig. 20 GARGAMELLE-quark and anti-quark momentum distributions.

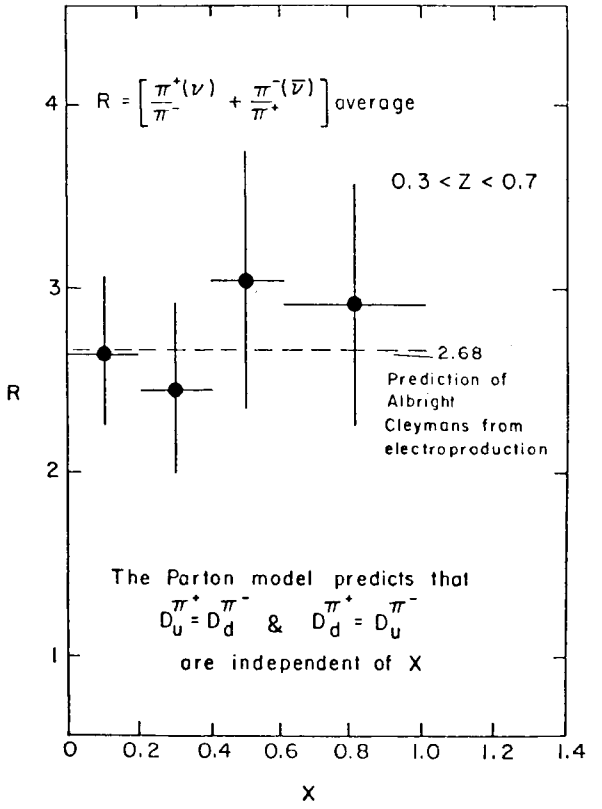

Fig. 21 GARGAMELLE-current fragmentation pion charge ratios.

Therefore, in conclusion to all the above analysis, though it is possible because of the low energy to doubt the physical interpretation of the data, it is a puzzle why there is such good agreement between the data and the quark-parton model predictions

3. SEARCH FOR NEW PARTICLES

3.1 Heavy Lepton Searches

During the past year the CALTECH group have continued to improve the lower mass limit for Georgi-Glashow type heavy leptons. The heavy lepton having the same lepton number as the ν_μ and μ^- would be detected by its decay into μ^+.

$$\nu_\mu + N \rightarrow Y^+ + \text{hadrons}$$
$$\hookrightarrow \mu^+ + \nu_\mu + \nu_\mu.$$

In a 170 GeV sign-selected beam, 1522 μ^- events and 8 μ^+ events were observed[22]. From the knowledge of the $\bar{\nu}_\mu$ contamination in the beam, all 8 μ^+ events could be attributed to $\bar{\nu}_\mu$ interactions.

The theoretical estimation of the branching ratio $\frac{Y^+ \rightarrow \mu^+ \nu\nu}{Y^+ \rightarrow \text{all}}$ is related to the branching ratio

$$R = \frac{e^+e^- \rightarrow \text{hadrons}}{e^+e^- \rightarrow \mu^+\mu^-}$$

As the latter ratio has not yet been seen to saturate the value of the lower limit at $M_Y > 7.2$ GeV at 90% C.L. (for $R = 10$, and equal couplings $G_F^2 = G_y^2$) can be probably considered a safe lower limit.

3.2 Charm Searches

The experimentally detectable signatures expected for charmed particle production would be a marked increase in single strange particle production, and consequently a change or step in the linear rise of the total cross-section.

3.2.1 GARGAMELLE Experiment

The GARGAMELLE group have looked[14] for associated and single strange particle production in ν film. In a heavy liquid chamber one is essentially blind to Σ^+, Σ^-, Σ^o and K^- production. Also there are large absorbtion effects which will also give rise to apparent cases of single strange particle production.

Due to these effects, the rate of associated strange particle production observed is certainly a lower limit, and that of single strange particle production an upper limit.

The results obtained were:

$$\left.\begin{array}{l} \sigma\ \dfrac{\text{associated production}}{\sigma\ \text{total}} > 0.5\% \\ \dfrac{\sigma_{\Delta s=1}}{\sigma\ \text{total}} < 2\% \end{array}\right\} > 90\%\ \text{C.L.}$$

The $\Delta s=1$ production in this experiment certainly cannot be considered anomalous. In addition, no evidence was found for any difference between the slopes of the total cross-sections for neutrinos coming from pions and kaons.

3.2.2 HPW Experiment

In an exposure using a ν_μ beam produced by 400 GeV protons, 300 charged current events were produced. In addition, two events which had both a μ^- and μ^+ coming from the same vertex were found[23]. The characteristics of these two events are given below:

	Event 1	Event 2
p_{μ^-}	107 GeV/c	36 GeV/c
p_{μ^+}	17 GeV/c	14 GeV/c
Hadronic Energy	24 GeV	105 GeV
Total Energy	147 GeV	155 GeV

The estimate of the background is $\sim 10^{-2}$. It would be very difficult to ascribe these events to the production of the intermediate boson. If they were W's, one should certainly not have expected a linearly rising total cross-section at FNAL energies. Also one would expect W's to be produced coherently and decay such that $p_{\mu^+} > p_{\mu^-}$.

They may however be due to the leptonic decay of some "new" unstable particle.

As these muon pairs are occurring at a rate of $\sim 1\%$, this group should soon be able to increase the statistics on these interesting events and shed a better light on their origin.

4. CONCLUSIONS ON CHARGED-CURRENT INTERACTIONS

(a) The behaviour of charged-current interactions is compatible with what one would expect from "scaling".

(b) The "precocious scaling" observed at low energy is surprising. It could be trivial, but it certainly needs an explanation.

(c) As yet no new particle has been "discovered". This does not exclude that many may have been produced.

4.1 Overall Conclusions

The field of neutrino physics is completely open and essentially unexplored!

ACKNOWLEDGEMENTS

I would like to thank the scientific secretaries W. Scott, S. Tovey and W. Venus for their assistance in preparing this review and also to B. Barish and G. Myatt for many helpful discussions.

REFERENCES

1. F.J. Hasert et al., Phys. Letters 46B (1973) 138 and Nucl. Phys. B73 (1974) 1.
2. F.J. Hasert et al., Paper 1013.
3. A. Benvenuti et al., 6th International Symposium Bonn (1973) Paper 288 and Phys. Rev. Letters 32 (1974) 800.
4. B. Aubert et al., Phys. Rev. Letters 32 (1974) 1454 and Phys. Rev. Letters 32 (1974) 1457.
5. B.C. Barish et al., Paper 587.
6. A. Pais and S.B. Treiman, Phys. Rev. D6 (1972) 2700, E.A. Pachos and L. Wolfenstein, Phys. Rev. D7 (1973) 91.
7. L.M. Sehgal, Nucl. Phys. B65 (1973) 141.
8. G. t'Hooft, Phys. Letters 37B (1971) 195.
9. S. Barish et al., Paper 530 to be published in Phys. Rev. Letters.
10. C.H. Albright et al., Phys. Rev. D7 (1973) 2220.
11. D.C. Cundy et al., Paper 1024.
12. D.C. Cundy et al., Phys. Letters 31B (1970) 439.
13. W. Lee et al., post dead-line paper.
14. GARGAMELLE Collaboration, Pyper 513.
15. B.C. Barish et al., Paper 588.
16. B. Aubert et al., Paper 691.
17. B.C. Barish et al., Paper 586.
18. B. Aubert et al., Paper 694.
19. D.J. Gross, C.M. Llewellyn-Smith, Nucl. Phys. B14 (1969) 337.
20. R. Mc. Elhaney and S.F. Tuan, Phys. Rev. D8 (1973) 2267. G. Altarelli et al., CERN Th.1757 (1974).
21. G.H. Albright and T. Cleymans, CERN Th.1829 (1974).
22. B.C. Barish et al., Paper 589
23. B. Aubert et al., Paper 693.